

# Critical Unmixing of Polymer Solutions

Helge Frauenkron<sup>1</sup> and Peter Grassberger<sup>1,2</sup>

<sup>1</sup> HLRZ c/o Forschungszentrum Jülich, D-52425 Jülich, Germany

<sup>2</sup> Physics Department, University of Wuppertal, D-42097 Wuppertal, Germany

August 1, 2021

## Abstract

We present Monte Carlo simulations of semidilute solutions of long self-attracting chain polymers near their Ising type critical point. The polymers are modeled as monodisperse self-avoiding walks on the simple cubic lattice with attraction between non-bonded nearest neighbors. Chain lengths are up to  $N = 2048$ , system sizes are up to  $2^{21}$  lattice sites and  $2.8 \times 10^5$  monomers. These simulations used the recently introduced pruned-enriched Rosenbluth method which proved extremely efficient, together with a histogram method for estimating finite size corrections. Our most clear result is that chains at the critical point are Gaussian for large  $N$ , having end-to-end distances  $R \sim \sqrt{N}$ . Also the distance  $T_\Theta - T_c(N)$  (where  $T_\Theta = \lim_{N \rightarrow \infty} T_c(N)$ ) scales with the mean field exponent,  $T_\Theta - T_c(N) \sim 1/\sqrt{N}$ . The critical density *seems* to scale with a non-trivial exponent similar to that observed in experiments. But we argue that this is due to large logarithmic corrections. These corrections are similar to the very large corrections to scaling seen in recent analyses of  $\Theta$ -polymers, and qualitatively predicted by the field theoretic renormalization group. The only serious deviation from this simple global picture concerns the  $N$ -dependence of the order parameter amplitudes which disagrees with a minimalistic ansatz of de Gennes. But this might be due to problems with finite size scaling. We find that the finite size dependence of the density of states  $P(E, n)$  (where  $E$  is the total energy and  $n$  is the number of chains) is slightly but significantly different from that proposed recently by several authors.

# 1 Introduction

Consider long flexible polymers in a not too good solvent. At high temperatures, they will form extended random coil configurations which can be modeled by self avoiding random walks. When  $T$  is lowered, there will be a critical temperature  $T_c$  where the chains start to coagulate and the liquid unmixes. This  $T_c$  increases with chain length  $N$ . At the *theta temperature* defined as  $T_\Theta = \lim_{N \rightarrow \infty} T_c(N)$  also a single (but infinitely long) chain will collapse. Qualitatively, this unmixing is described by the mean field theory developed by Flory and Huggins [1]. The phase diagram is sketched in fig.1.

For any finite  $N$  we expect that the internal structure of the dissolved “particles” (=chains) becomes irrelevant in the infrared limit, i.e. close to  $T_c(N)$ . Thus, the critical behavior should be fully described by the Ising model, i.e. by the  $O(n)$  sigma model with  $n = 0$  [2, 3]. This is indeed supported by all available evidence, but it tells only half of the story. As in any critical phenomenon there are universal and non-universal properties. While the (Ising-)universal aspects (critical exponents and scaling functions) must be independent of  $N$ , all non-universal parameters should depend on  $N$  systematically, and can be expected to display another type of scaling in the limit  $N \rightarrow \infty$ . Also, the critical region must become smaller and smaller as  $N$  is increased, and there must be a cross-over to the critical behavior holding at the  $\Theta$  point. The latter is formally described by a tricritical point in the  $O(n)$  model with  $n = 0$ . As any tricritical point in  $O(n)$  models, its upper critical dimension is  $d = 3$ , whence it should display mean field behavior with logarithmic corrections [2].

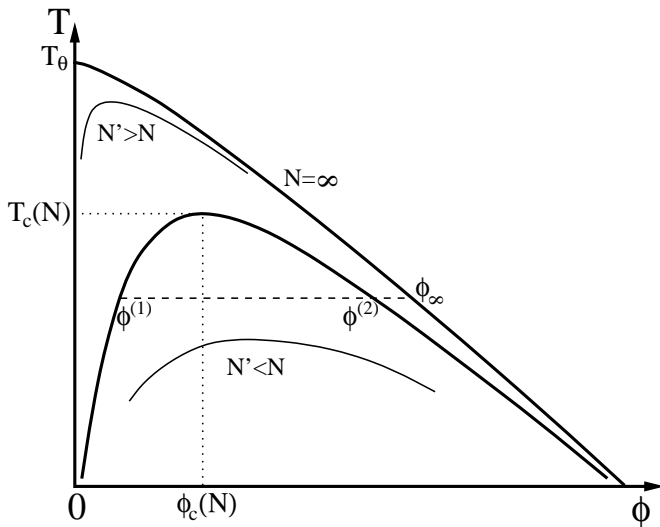


Figure 1: Schematic phase diagram for semi-dilute solutions of chain polymers. The uppermost curve gives the monomer concentration inside an infinitely large collapsed globule under zero outside pressure. The lower curves are coexistence curves for fixed chain length  $N$ . These curves are strictly monotonically ordered, with the coexistence curve for  $N$  below that for  $N'$  if  $N < N'$ .

The cross-over should be described by scaling laws which are accessible to experiment, but which cannot yet be obtained fully from the field theoretic renormalization group. Thus even the basic critical exponents are not known, and are the subject of controversial speculations. The main theoretical difficulty is that the Ising transition and the  $\Theta$ -collapse have different upper critical dimensions, making an  $\epsilon$ -expansion non-trivial.

Let us denote the monomer density by  $\phi$ . In Flory-Huggins theory one assumes that the entropy per unit volume is given by [2]

$$S = -\frac{\phi}{N} \ln \frac{\phi}{N} - (1 - \phi) \ln(1 - \phi) , \quad (1)$$

and the energy is a quadratic function of  $\phi$  independent of  $N$ . Keeping only the mixing entropy, expanding  $\ln(1 - \phi)$  in powers of  $\phi$ , and dropping the irrelevant linear term in  $\phi$ , the free energy per unit volume is thus given by

$$\beta F = \frac{\phi}{N} \ln \phi + \frac{1}{2}v\phi^2 + \frac{1}{6}w\phi^3 + \dots . \quad (2)$$

The  $\Theta$  point corresponds to a vanishing of  $v$ . We assume that  $v$  is a linear function of  $T$ , while  $w > 0$  is constant. All (mean field) scaling laws can be obtained from this ansatz. In particular, the critical density and the distance from the  $\Theta$  point both turn out to scale as  $N^{-1/2}$ ,

$$\phi_c \sim 1/\sqrt{N} \quad (3)$$

and

$$T_\Theta - T_c(N) \sim 1/\sqrt{N}. \quad (4)$$

For  $N = \infty$ , the density at  $T < T_\Theta$  scales linearly as

$$\phi_\infty \sim T_\Theta - T. \quad (5)$$

Unfortunately, the theory – being mean field – predicts also the classical value  $1/2$  for the order parameter exponent  $\beta$ . For finite  $N$ , the density difference along the coexistence curve (the ‘order parameter’) is predicted to satisfy a scaling law

$$\phi^{(2)} - \phi^{(1)} = N^{-1/2} f((T_c - T)\sqrt{N}) \quad (6)$$

with  $f(x) \sim \sqrt{x}$  for  $x \rightarrow 0$ , and  $f(x) \sim x$  for  $x \rightarrow \infty$ . A minimal modification which gives the correct value of  $\beta$  ( $\approx 0.325$ ) was proposed by de Gennes [2]. He suggested to keep eqs.(3) to (6), and to adopt simply a different behavior for  $f(x)$ :

$$f(x) \sim x^\beta , \quad x \rightarrow 0 . \quad (7)$$

This ansatz seems theoretically consistent although it cannot be derived from an underlying microscopic theory. But unfortunately eq.(3) is in serious conflict with experiment. Most experiments [4, 5, 6, 7, 8] and subsequent analyses [9, 10, 11, 12] agree that

$$\phi_c \sim N^{-x_2} \quad (8)$$

with

$$x_2 = 0.38 \pm 0.01 . \quad (9)$$

This discrepancy has given rise to a number of speculations and more or less well founded conjectures [10, 11, 13, 14, 15, 16, 17]. One conjecture is that the chains might be partly collapsed at the critical point. Since  $T_c(N) \rightarrow T_\Theta$  for  $N \rightarrow \infty$ , the natural first assumption is that the end-to-end distance or the radius of gyration should scale as  $R \sim \sqrt{N}$ , i.e. the chains should be free. One might question this since actually  $T_c(N) < T_\Theta$  for any finite  $N$ . Accordingly, it was suggested in [16] that chains are partly collapsed,

$$R_N \sim N^{x_0} \quad (10)$$

with an exponent  $x_0 < 1/2$ . Actually, this is most unlikely. On the one hand, the effective collapse temperature for finite  $N$  – defined as that  $T$  where  $R_N$  is the same value as for ideal chains – is below  $T_\Theta$  [21]. On the other hand, chains must be in contact at the critical point (otherwise they would not interact) and can penetrate each other. Thus there is no force which should compress them beyond the ideal shape which maximizes entropy. This argument is very similar to that which explains why chains in dense melts are basically ideal.

In spite of these doubts, it seems wise to leave the exponents eqs.(8) and (10) open at the present point, and to assume similar scaling laws also for the other observables:

$$\phi^{(2)} - \phi^{(1)} \sim (T_c - T)^\beta N^{-x_1} \quad (11)$$

and

$$T_\Theta - T_c(N) \sim N^{-x_3} . \quad (12)$$

Notice that eqs.(6) and (7) would give  $x_1 = (1 - \beta)/2 \approx 0.34$ . Experimentally, the exponents are [3, 18]

$$x_1 \approx 0.23 - 0.34 , \quad x_3 \approx 0.47 - 0.5. \quad (13)$$

In addition, we can generalize eq.(5) to

$$\phi_\infty \sim (T_\Theta - T)^y \quad (14)$$

with some unknown exponent  $y$ , although it seems that *all* authors have assumed that  $y = 1$ , with a single exception to be discussed below.

Since the  $\Theta$ -point is a tricritical point, one should expect logarithmic corrections to these scaling laws [19, 20]. To leading order, they are obtained by replacing  $v$  and  $w$  in eq.(2) by their renormalized values for large  $N$ ,

$$v \rightarrow \text{const} (T - T_\Theta)[\ln N]^{-4/11}, \quad w \rightarrow \text{const}/\ln N. \quad (15)$$

Among others this gives [19]

$$\phi_c \sim \frac{[\ln N]^{1/2}}{\sqrt{N}} \quad (16)$$

and

$$T_{\Theta} - T_c(N) \sim N^{-1/2} [\log N]^{-3/11}, \quad (17)$$

From this follows  $\phi_c \sim (T_{\Theta} - T_c) [\log(T_{\Theta} - T)]^{7/11}$ .

Similar corrections are predicted for the end-to-end distance of single chains at the  $\Theta$ -point, for the specific heat, and for other observables [20] (but not for pure Ising properties such as  $\phi^{(2)} - \phi^{(1)}$ ). These corrections for single chains are not (yet) fully seen in simulations. More precisely, simulations [21, 22] show for most observables corrections which are much larger than those predicted by theory, with only weak hints that the theoretical predictions are correct for extremely large  $N$  [22].

One such case where corrections to mean field behavior are very large is the dependence of  $\phi_{\infty}$  on  $T_{\Theta} - T$ . Based on simulations of very long chains, it was shown in [21] that a best fit is given by  $y = 0.7$ . But using even longer chains, with  $N$  up to  $10^6$ , it was concluded in [22] that this is an effect of very large corrections to scaling, and that  $y = 1$  is indeed the most likely value. Indeed, as shown in [19], one expects logarithmic corrections with the same power as for  $\phi_c$ ,

$$\phi_{\infty} \sim (T_{\Theta} - T) [\log(T_{\Theta} - T)]^{7/11}. \quad (18)$$

Let us forget for the moment any logarithmic corrections, and assume that the scaling laws (8) - (14) hold. We should point out that the exponents  $x_i$  and  $y$  are not independent. A simple argument gives

$$x_3 y \leq x_2. \quad (19)$$

To derive this, one just needs that  $\phi_c(N) \leq \phi_{\infty}$  at fixed temperature  $T = T_c(N)$ . But this follows from the fact that phase coexistence regions grow with  $N$ : if the point  $(T, \phi)$  is in the phase coexistence region for some  $N$ , it is also in this region for all  $N' > N$  (we have not found a mathematically rigorous proof for this, but it seems heuristically obvious, and it was assumed tacitly by all previous authors).

Inserting  $y = 1$  and the numerical values (9) and (13), we see that eq.(19) is violated. It seems that this simple observation has been overlooked in all recent literature, and it makes several claims obsolete. One either has to admit that  $y < 1$ , or that  $x_2$  is much closer to its mean field value than suggested by experiments, or (which seems the least likely) that  $x_3$  deviates strongly from its mean field value.

In view of this unclear situation we decided to perform large scale simulations using a novel Monte Carlo algorithm, the Pruned-Enriched Rosenbluth Method (PERM) [22]. We refer to this reference and to sec.2 for a description of this algorithm. It allowed us to simulate very large systems, with chains of length up to 2000 and beyond. Indeed, we could have gone even further as concerns chain length, but we had problems going to systems containing more than  $\approx 400$  chains, even if these chains are short. This is due to the fact that PERM performs excellently at the  $\Theta$ -point, but becomes less efficient at temperatures much below  $T_{\Theta}$ . The latter is needed for simulations of short chains at the critical point.

Thus all our simulations were done on lattices with finite volume  $V$  in a regime where finite size corrections are important. To perform a detailed finite size analysis, we used the histogram method as proposed in [23, 24], and applied to polymers in [18]. In this method, one constructs the microcanonical distributions<sup>1</sup> (“histogram”)  $P(E, n)$  where  $E$  is the energy and  $n$  is the number of chains. Ising universality requires that  $P(E, n)$  has certain scaling properties which can be used to extrapolate to the thermodynamic limit. In the Ising model proper (which is just the  $N = 1$  limit of the lattice polymer model studied below),  $2nN/V - 1$  is replaced by the magnetization  $M$ , and  $P(E, M)$  is symmetric under  $M \rightarrow -M$ . This symmetry is broken for  $N > 1$ , but restored at the critical point (i.e., for  $E \approx E_c$  and  $n \approx n_c$  in the thermodynamic limit). It was claimed in [23, 24, 18] that the dominant symmetry breaking term in the vicinity of  $(E_c, n_c)$  can be removed by an affine transformation

$$\mathcal{E} = E - rn, \quad \mathcal{N} = n - sE \quad (20)$$

with  $N$ -dependent parameters  $r$  and  $s$  (“field mixing” [25]). We found that this is not true in our case. Although parameters  $r, s$  can be found such that the marginal distributions  $P(\mathcal{N})$  and  $P(\mathcal{E})$  agree with the Ising universal curves within error bars (implying also that  $P(\mathcal{N})$  is symmetric around  $\mathcal{N}_c$ ), the 2-dimensional distribution does not become more symmetric by this transformation. Nevertheless, the possibility to compare with the precisely known critical magnetization distribution of the Ising helps enormously in fixing the critical point, and extracting critical parameters. We thus basically verified that the histogram method gives very reliable (and large!) finite size corrections, allowing us to obtain precise critical parameters from fairly small system sizes.

The algorithm and computational details are discussed in the next section. In sec.3 we describe the histogram method, and our main results are presented in sec.4. One interesting aspect of PERM is that it allows to compute free energies with high precision. We use this to compare directly with the mean field ansatz eq.(2). We conclude with a discussion of our results in sec.5.

## 2 Algorithm and Computational Aspects

The Pruned-Enriched Rosenbluth Method (PERM) [22] is a chain growth algorithm based on the Rosenbluth-Rosenbluth (RR) method [26] and on “enrichment” [27] or copying of successful partial chains. As is well known [28], the main drawback of the RR method is that it leads to weighted samples with very uneven weights. This is counterbalanced in PERM by enrichment (when a large weight chain is copied  $k$  times, all  $k + 1$  copies receive  $1/(k + 1)$  times the original weight) and by *pruning*: low weight chains are either pruned (deleted) or, with the same probability, doubled in weight. Similar algorithms have been used in [29, 30]. There, however, they were implemented

---

<sup>1</sup>Strictly spoken,  $P(E, n)$  is the microcanonical partition sum multiplied by  $e^{-\beta(E-\mu n)}$ , and normalized so that  $\sum_{E, n} P(E, n) = 1$ .

in a ‘breadth first’ way, by keeping a large population of chains simultaneously in memory. Such a strategy would have been not feasible for the very large systems (up to several hundred thousand monomers) treated in this paper. Instead, we used a recursive ‘depth first’ strategy. The basic algorithm is described in detail in [22], some further tricks to make it faster and more robust are discussed in [31, 32]. We refer to these papers for details. We just mention that we hand-coded the recursion without using recursive function calls, in contrast to the algorithm shown in the appendix of [22], since we otherwise would have had problems with storage. All simulations reported in this paper were done on workstations and used less than 50 MB main memory.

As designed originally, PERM applies to classical (distinguishable) particles which are tied together to form a chain polymer. To simulate systems with several polymer chains which are indistinguishable and not connected, we need some modifications. The first is that each time when we start a new chain, we have to choose the location of its first monomer anywhere in the not yet occupied volume. For the  $k$ -th chain in volume  $V$ , this implies a Rosenbluth factor  $V - (k - 1)N$ . The total Rosenbluth weight for a system consisting of  $n$  chains is then  $\prod_{k \leq n} (V - (k - 1)N)$  times the product of proper Rosenbluth factors for the second, third, ...  $N$ -th monomers in the chains. Secondly, we have to multiply the final weight by  $1/n!$  since there are exactly  $n!$  possibilities to build up a configuration of  $n$  chains sequentially.

In PERM one uses the product of Rosenbluth and Boltzmann weights of partially assembled systems to steer doubling and pruning. In order to have a smooth dependence of the doubling and pruning thresholds on the number of already assembled monomers, we omitted the above factors during the growth, and added them later when the system was already built up.

All simulations were done on the simple cubic lattice with helical boundary conditions (lattice sites are indexed by a single integer  $i$ , and  $i + V \equiv i$ ). Chains were modeled by self-avoiding walks with attractive energy  $\epsilon = -1/k_B$  between each pair of neighboring non-bonded monomers. Chain lengths were powers of 2. Volumes were also powers of two,  $V = 2^m$  with  $m$  such that systems at the critical point had roughly 100 chains. Thus  $V$  changed from  $2^{12}$  for  $N = 8$  to  $2^{21}$  for  $N = 2048$ . CPU times (on DEC Alpha machines with 400 Mhz) ranged from a few hours for  $N = 8$  to roughly two weeks for  $N = 2048$ .

In these simulations we used one constant chemical potential  $\mu$  for each chain, and another potential  $\mu'$  for each monomer. Since we measured observables only after chains had been finished, this corresponds to an overall fugacity  $z = e^\mu e^{N\mu'}$  per chain. We measured:

- The canonical partition sum  $Z_n$  for each  $n = 1, 2, \dots, n_{\max}$ . This is needed anyhow for the control of doubling and pruning.
- The average energy  $E_n$  of the total configuration containing  $n$  chains,  $n = 1, 2, \dots, n_{\max}$ .
- The average energy  $e_n$  of the  $n$ -th inserted chain at the moment of its insertion. Notice that  $E_n$  is approximately equal to  $\sum_{k=1}^n e_k$ , but not exactly.

- The average r.m.s. end-to-end distance  $R_{N,n}$ , averaged over all chains.
- The end-to-end distance  $r_{N,n}$  for the last inserted chain. Again,  $R_{N,n}$  is approximately but not exactly equal to  $r_{N,n}$ .
- A histogram which contains for each pair  $(E, n)$  the microcanonical partition sum multiplied by  $e^{-\beta E} z^n$ .

We do not present results for chains shorter than  $N = 8$ , mainly because this requires simulations at rather low temperatures. The algorithm becomes inefficient there. For instance, for the Ising model ( $N = 1$ ) we had no problems to simulate lattices of size  $4^3$ , verifying thereby that the algorithm works in principle also on this extreme case. But already for systems with  $V = 8^3$  we encountered problems. This is not too surprising. In spin language, we start simulations with all spins down. We chose random sites where spin is still down and flip it up, keeping track of the Boltzmann weights by giving each configuration a weight different from 1. If this weight becomes too large or too small, we copy or prune, respectively. Finally, if pruning did not kill us, we end up at the configuration with all spins up. The total weight of this state should be the same as that of the starting configurations with all spins down. While this symmetry is exactly respected by the Rosenbluth method without pruning or copying, it is not by PERM due to the stochastic nature of pruning. In the long run, of course, the symmetry will be approached closer and closer. But this is due to very rare events with very large weights. It not only involves huge statistical errors but also a systematical bias unless one is very careful and does not estimate statistical errors from fluctuations within small samples. These problems have to be kept in mind when dealing with  $N > 1$ . In this case there is no symmetry to check, but there is the same danger of underestimating the contribution of rare outliers. We hope to have minimized this danger by using very large samples, typically  $10^6$  to  $10^7$  independent “tours” in the terminology of [22].

### 3 Histogram Method and Finite Size Scaling

Let us consider for the moment an Ising system in  $d$  dimensions with lattice size  $L$ . We denote by  $\mathcal{Z}_L(T, h)$  the canonical partition sum, and by  $Z_L(E, M)$  the number of states with energy  $E$  and magnetization density  $M$ . The *histogram*  $P_L(E, M)$  is defined as

$$P_L(E, M) = \frac{e^{-\beta E + h L^d M}}{\mathcal{Z}_L(T, h)} Z_L(E, M) . \quad (21)$$

For vanishing external magnetic field  $h$  and at  $T = T_c$  it should scale as [23, 24]

$$P_L(E, M) \approx L^{\beta/\nu - 1/\nu} g(L^{\beta/\nu} M, (E - E_c)L^{-1/\nu}) \quad (22)$$

where  $E_c$  is the average energy at the critical point, and  $\beta = 0.327 \pm 0.001$  and  $\nu = 0.630 \pm 0.001$  [33, 34] are the usual critical indices. The function  $g$  is universal up to

rescalings of its value and arguments by arbitrary factors. Summing over  $E$  resp.  $M$  we obtain the distributions of magnetization resp. energy,

$$P_L(M) \approx L^{\beta/\nu} \tilde{p}_M(L^{\beta/\nu} M) \quad (23)$$

and

$$P_L(E) \approx L^{-1/\nu} \tilde{p}_E((E - E_c)L^{-1/\nu}) . \quad (24)$$

The energy scaling function  $\tilde{p}_E(x)$  has a single maximum. In contrast, the magnetic scaling function  $\tilde{p}_M(x)$  has two (symmetric) maxima for  $d < 4$ .

This is the main point which a finite size scaling analysis has to take into account correctly. Naively, the critical point is defined as that temperature where  $\tilde{p}_M(x)$  changes from being single-humped to double-humped. But strictly, this is true only in the thermodynamic limit, and analyses which neglect this when estimating  $T_c$  [35, 36, 37] can have very large systematic errors. More precisely, in  $d = 3$  the ratio  $\tilde{p}_M(0)/\max_x \tilde{p}_M(x)$  is roughly 0.44, with an error probably  $< 0.02$  [24]. In the  $(E, M)$ -plane, the distribution  $P_L(E, M)$  at  $h = t = 0$  has two peaks located on the two halves of a U-shaped support.

Let us now consider a system like a critical gas where  $M$  is replaced by the particle density  $\rho (= \phi/N)$ , and the symmetry  $M \rightarrow -M$  is lost. In the following we shall use the total particle number  $n$  instead of  $\rho$ . According to [23, 24], one just has to replace  $E$  and  $n$  by linear combinations

$$\mathcal{E} = E - r n \quad (25)$$

and

$$\mathcal{N} = n - s E \quad (26)$$

with suitable constants  $r$  and  $s$ . One arrives at scaling laws for  $\mathcal{E}$  and  $\mathcal{N}$  which formally coincide exactly with eqs.(22-24) except for the fact that also  $\mathcal{N}_c = \langle \mathcal{N} \rangle$  is different from zero and that  $\mathcal{N} - \mathcal{N}_c$ , being an extensive quantity, replaces not  $M$  but  $L^d M$ :

$$P_L(\mathcal{E}, \mathcal{N}) \approx L^{\beta/\nu - 1/\nu - d} g((\mathcal{N} - \mathcal{N}_c)L^{\beta/\nu - d}, (\mathcal{E} - \mathcal{E}_c)L^{-1/\nu}) . \quad (27)$$

This conjecture was tested in [23, 24, 18] mainly by verifying that the projected 1-dimensional distributions  $\tilde{p}_L(\mathcal{N})$  and  $\tilde{p}_E(\mathcal{E})$  agreed numerically with the Ising scaling functions. For polymer solutions we expect  $r$  and  $s$  to scale with  $N$  in a universal way.

Notice that the justifications for eqs.(25) and (26) are rather different. Replacing the energy density  $E$  by a linear combination  $E - r n$  just corresponds to changing the internal energy of the particles. Since that is arbitrary anyhow, we see that eq.(25) is very natural. It just corresponds to a shift in the internal energies such that both phases have the same energy density per unit volume. No such interpretation can be given for eq.(26).

Let us assume that we have made the simulations at a temperature near  $T_c$ . We first obtain rough estimates of the critical fugacity  $z_c$  and of  $r$  by demanding that both peaks in  $P_L(n)$  have the same height, and that the two peaks in  $P_L(\mathcal{E}, n)$  occur at the same value of  $\mathcal{E}$ . A typical result, for  $N = 128$ , is shown in fig.2a. By summing

over all  $E$ , we obtain the chain number distribution shown in fig.3a. Notice the very asymmetric shape of both distributions. Notice also that the ratio between the height of the central minimum of  $P_L(n)$  and its maximal value is not exactly 0.44, indicating that we have not simulated exactly at  $T_c$ .

In a first refinement we now determine a crude estimate of  $T_c$  by re-weighting  $P_L(\mathcal{E}, n)$  such that the minimum in the projected distribution  $P_L(n)$  has a height equal to 0.44 times the average value of the maxima. We then fit  $s$  such that  $P_L(\mathcal{N})$  becomes symmetric under  $\mathcal{N} - \mathcal{N}_c \rightarrow -(\mathcal{N} - \mathcal{N}_c)$ , where  $\mathcal{N}_c$  is the minimum position, and readjust at the same time the fugacity  $z_c$  such that both peaks have again the same height. The fact that we always do find a value of  $s$  such that  $P_L(\mathcal{N})$  becomes approximately symmetric and equal to the Ising scaling function is highly non-trivial.

The last readjustment will in general have shifted the peaks in the  $(\mathcal{E}, \mathcal{N})$ -plane such that they occur no longer at the same value of  $\mathcal{E}$ . We thus repeat the fit of  $r$  and estimate more precise values of  $T_c$ ,  $z_c$ , and  $s$  by repeating the second step. In principle, we could iterate this procedure until we reach convergence, but already after the second refinement the two peaks of  $P_L(\mathcal{E}, \mathcal{N})$  will occur at the same  $\mathcal{E}$ . We then check that  $P_L(\mathcal{N})$  and  $P_L(\mathcal{E})$  agree with the scaling functions given in [24] within the statistical errors. The final results for the raw data shown in figs.2a and 3a are shown in figs. 2b and 3b. For other chain lengths, results are very similar.

We thus have succeeded in finding field mixings such that the 1-d projections of the 2-d histogram agree with the Ising case. Exactly this was done also in [23, 24, 18]. But we see from fig.2b that the symmetry of the projected density  $P_L(\mathcal{N})$  is misleading. The 2-d histogram has not become more symmetric by replacing  $n$  by  $\mathcal{N}$ . We have not tried to apply formal measures of symmetry to fig.2, but it seems that fig.2b is rather less symmetric than fig.2a.

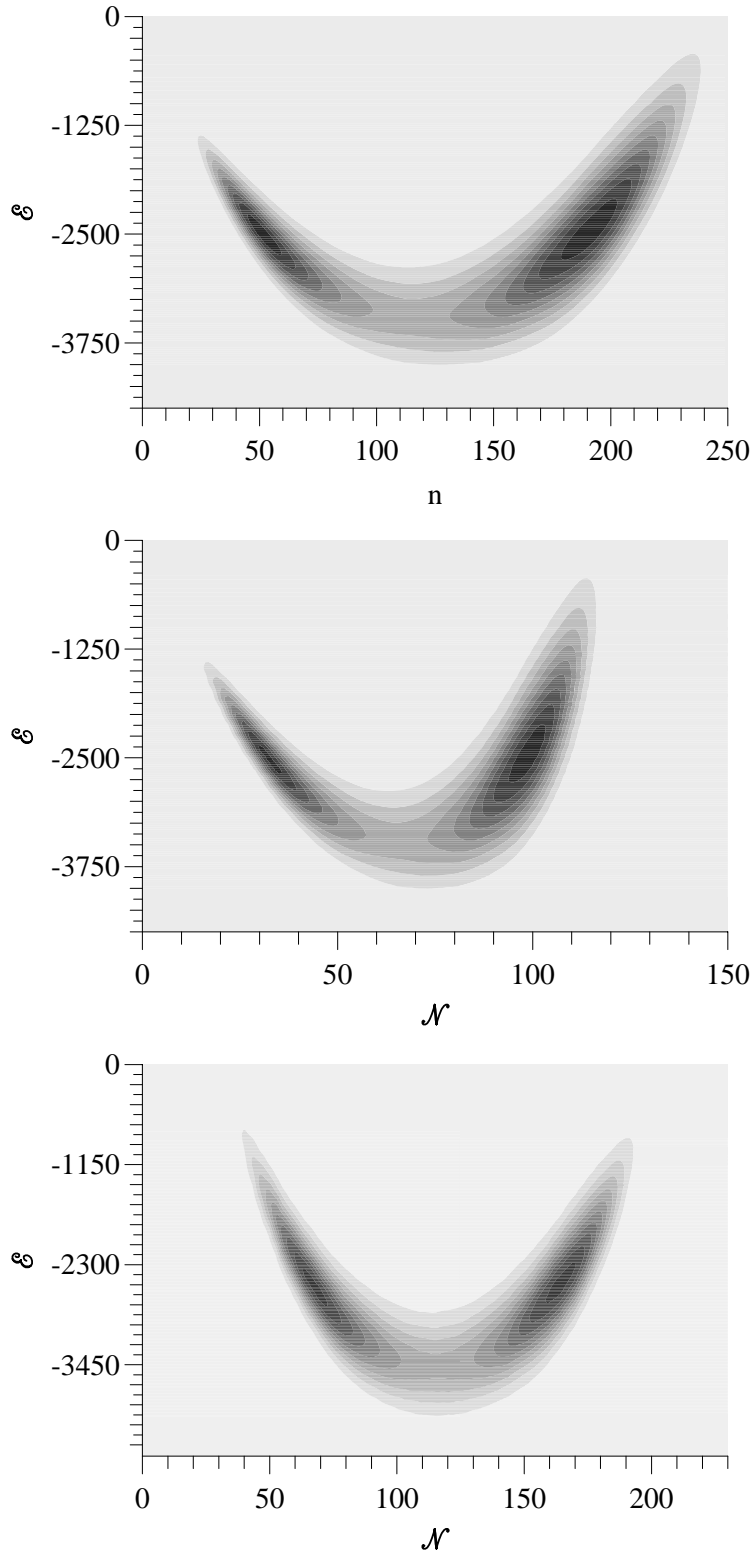
We see thus that linear field mixing is questionable. We tried a number of alternatives. By far the most successful numerically is the following. We first subtracted from  $E$  a term linear in  $n$  (corresponding just to a redefinition of internal energy), and then applied a conformal transformation with a scale factor which depends only on  $n$ . We did not try to optimize systematically since this is heuristic anyway, but good results were obtained with power law factors,

$$\mathcal{N} = (n/\langle n \rangle)^\alpha n, \quad \mathcal{E} = (n/\langle n \rangle)^\alpha (E - r n). \quad (28)$$

The same data shown already in figs.2a and 2b are plotted against these variables in fig.2c, with  $\alpha = -0.3$ . We see indeed a much more symmetric distribution. One-dimensional projections from this distribution are not very different from those obtained with linear mixing, and are not shown.

These different mixing ansatzes showed us that the estimates of  $T_c$ ,  $n_c$  and of the critical fugacity are very robust. Heuristically, this can be explained by the fact that the support of  $P_L(E, n)$  is a very narrow band, i.e. the variance of  $E$  for fixed  $n$  is rather small. We thus conclude somewhat paradoxically that we cannot verify a basic assumption of [23, 24, 18], but we agree that the histogram method is extremely helpful for extracting critical parameters.

Figure 2: (a) Contour plot of  $P_L(\mathcal{E}, n)$  for chains of length  $N = 256$  in a lattice with size  $L = 64$ . Notice the asymmetric shape. For the Ising model, the contour plots would be symmetric under reflection on the vertical axis. The normalization is arbitrary. (b) Same data as in panel a, but after transforming  $n \rightarrow \mathcal{N}$  by means of eq.(26) and readjusting the other parameters. The parameter  $s$  is 0.003. (c) Same data again, but using the non-linear transformation eq.(28).



To verify the correctness of the approach (and of the simulations!), we checked the scaling with  $L$  for one chain length,  $N = 128$ . According to eq.(23), the values of  $L^{-\beta/\nu} P_L(\mathcal{N})$  should coincide when plotted against  $L^{\beta/\nu} \mathcal{N}$ . This scaling plot is shown

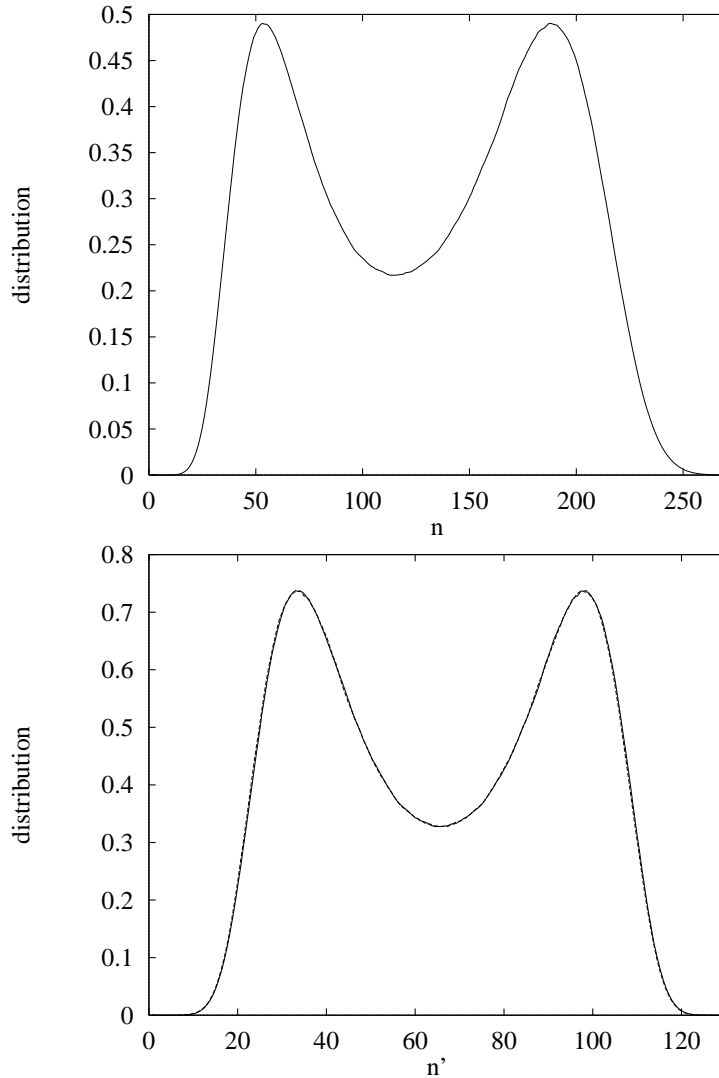


Figure 3: (a) Distribution  $P_L(n) \equiv z^n Z_n$  (up to an arbitrary normalization factor) against  $n$ , obtained by projecting the density of fig.2 onto the horizontal axis. (b) Same as panel a, but after transforming  $n \rightarrow \mathcal{N}$ . To demonstrate the symmetry of the distribution, both curves  $P_L(\mathcal{N})$  and  $P_L(2\mathcal{N}_c - \mathcal{N})$  are superimposed. As in the previous figures, the normalization is arbitrary.

in fig.4a, while the analogous scaling plot for the energy distribution is shown in fig.4b. We see perfect agreement. For other chain lengths we usually simulated at two lattice sizes in order to check for obvious inconsistencies, but we did not check systematically the finite size scaling.

## 4 Results

As a first result we show the swelling factor  $R_N^2/N$  for three different temperatures as a function of the number  $n$  of chains (fig.5). These results were obtained at fixed  $L$

and  $N$ . The critical point corresponds to the central curve and to  $n_c \approx 79$ . From this we can make several interesting observations:

- 1) All chains are swollen, i.e.  $R_N > \sqrt{N}$  in all cases.
- 2) The swelling is weakest for  $n = 1$ , i.e. for isolated chains, and increases as the chain density is increased. For large  $n$  it seems to saturate at a value  $< 2$ . This agrees with the fact that all three temperatures are below the  $\Theta$  point, and chains at  $T_\Theta$  are slightly swollen, with  $R_N^2/N \rightarrow 1.7 - 2$  for  $N \rightarrow \infty$  [21, 22]. For large  $n$  the chains feel mainly the slight imbalance between self avoidance and attraction for short chains which makes them swollen like very long  $\Theta$  chains, but for small  $n$  the attraction from the other chains is missing and the chains are slightly less swollen.
- 3) There is rather weak dependence on  $T$ , and this dependence weakens further as  $n$

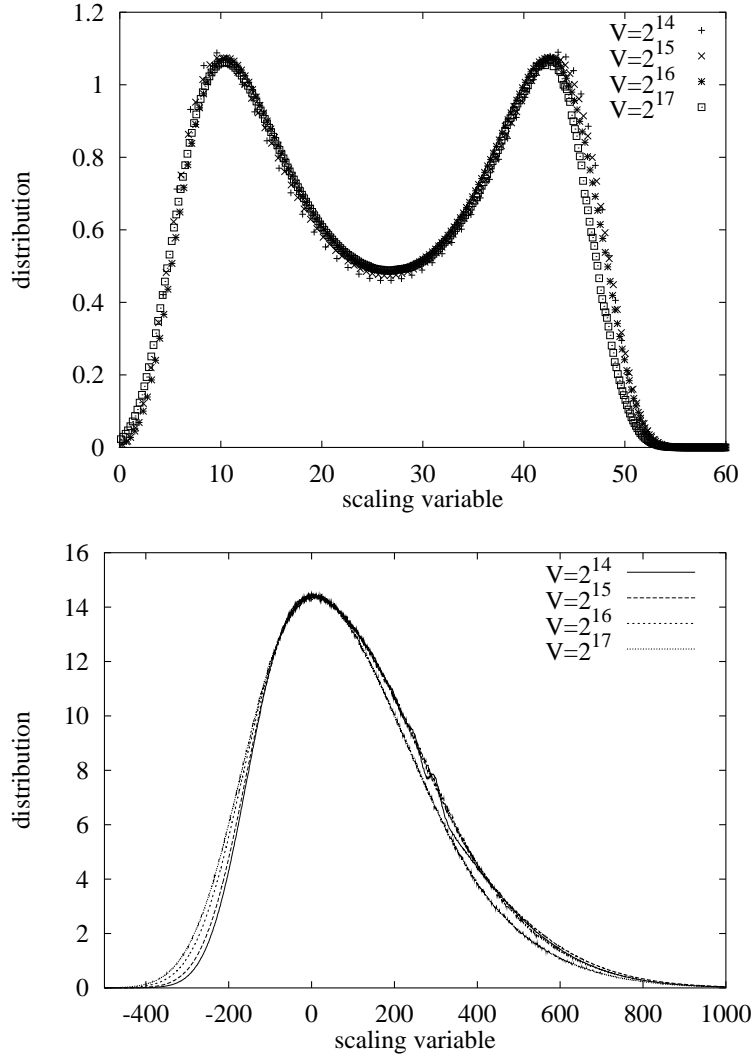


Figure 4: (a) Scaling plot of the distribution of transformed chain numbers  $\mathcal{N}$  for  $N = 128$  and  $T = 3.168$ . Within statistical errors, the latter is our estimate for  $T_c$ . The critical monomer density was assume to be  $\phi_c = 0.1544$ . (b) The analogous distribution of the transformed energy  $\mathcal{E}$ .

increases.

As a result of the last point, the systematic uncertainty in  $R_N^2/N$  due to the uncertainty of  $T_c$  is negligible. Not negligible, in contrast, is the dependence on the estimate of  $n_c$ . Indeed, due to the very small statistical errors in fig.5, the uncertainty of  $n_c$  is the largest source of error for  $R_N$ .

Results for  $R_N^2/N$  at the critical point obtained from fig.5 and from similar figures for other values of  $N$  are shown in fig.6. We see that the swelling increases slightly with  $N$ , as also found in [18]. But in contrast to these authors we see that the swelling saturates, ruling out a growth of  $R_N$  with a power  $> 1/2$ . Of course, such a growth would seem very strange and was rejected on this ground in [18]. But we can even extrapolate to  $N = \infty$  (dashed curve in fig.6), and verify that we obtain in this limit the same swelling as for isolated  $\Theta$  polymers.

To estimate the exponent  $x_1$  directly, one would have to simulate much larger systems than we could afford. But one can obtain this exponent indirectly from finite-size scaling exactly at  $T_c$ . Let us denote by  $\Delta\mathcal{E}$  and  $\Delta\mathcal{N}$  the rms widths of  $p_L(\mathcal{E})$  and  $p_L(\mathcal{N})$ , respectively. Keeping the  $N$ -dependent non-universal factors omitted in eq.(27), one easily shows that

$$\phi^{(2)} - \phi^{(1)} \sim (T_c - T)^\beta \frac{N}{L^d} \Delta\mathcal{N} [\Delta\mathcal{E}]^\beta. \quad (29)$$

We tried to use this for estimating  $x_1$ . But the results were rather disappointing, presumably because of the uncertainty in the field mixing. In the linear mixing ansatz, eqs.(25,26) were actually written in [23, 18] as a map  $(\mathcal{E}, \mathcal{N}) = (1-rs)^{-1}(E-rn, n-sE)$ . We have omitted the factor  $(1-rs)^{-1}$  up to now since it is irrelevant for everything we did up to now, but it does become relevant in eq.(29). But we also had argued that

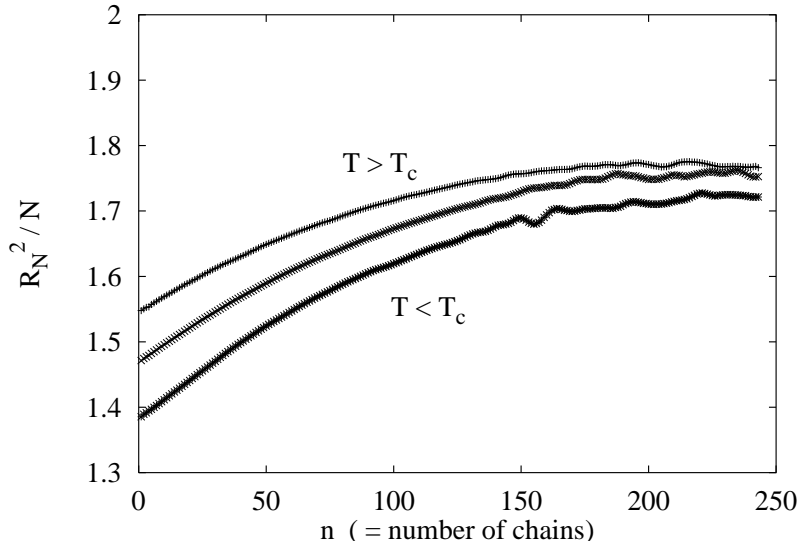


Figure 5: Swelling factors  $R_N^2/N$  for fixed  $N = 128$  at three temperatures,  $T = 3.03, 3.1655,$  and  $3.30$  (bottom to top), plotted against the number of chains  $n$ . The central value is close to the estimated  $T_c$ . All data were obtained with  $L^3 = 2^{16}$  sites.

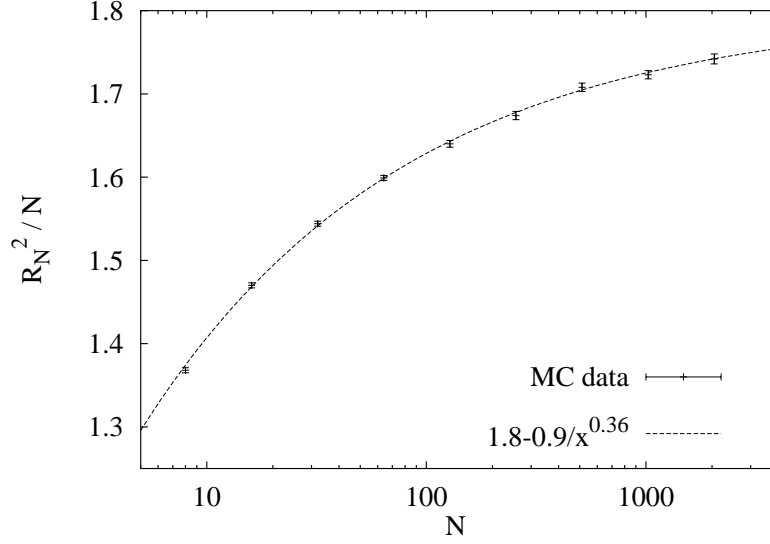


Figure 6: Swelling factors at the critical point against  $N$ . The dashed line is a fit with the function  $1.8 - 0.9x^{-0.36}$ . This fit has no particular significance except for the fact that the limit  $N \rightarrow \infty$  agrees with the swelling of infinitely long  $\Theta$  polymers.

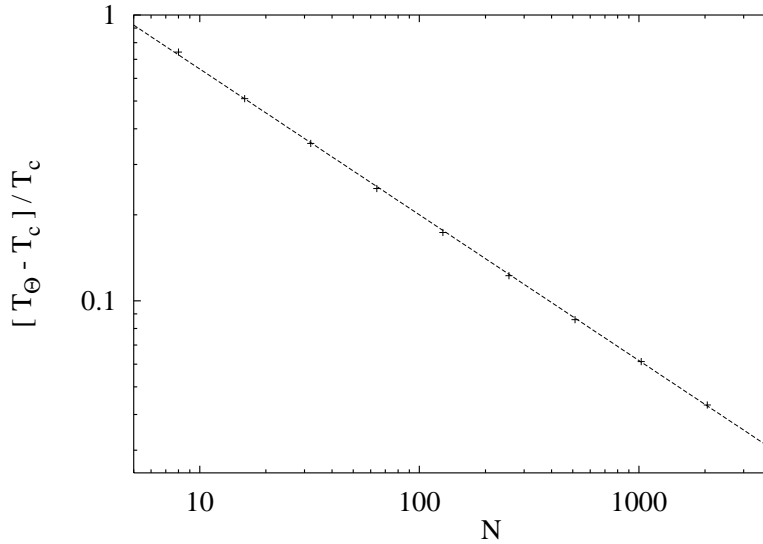


Figure 7: Log-log plot of  $(T_\Theta - T_c(N))/T_c(N)$  against  $N$  (crosses). The dashed line has slope  $-0.51$ .

eq.(25) is very natural as it is written, without the factor  $(1 - rs)^{-1}$ . Thus we propose that the correct linear mixing for our purpose is

$$\mathcal{E} = E - r n, \quad \mathcal{N} = (1 - rs)^{-1}(n - s E) = n - \frac{s}{1 - rs}\mathcal{E}. \quad (30)$$

Using this, we obtain  $x_1 \approx 0.18$ , albeit with large error bars which are hard to estimate

since they are a mixture of statistical and systematic errors.

Alternatively, we also tried the nonlinear transformation eq.(28), and we tried to use the untransformed width  $\Delta n$  instead of  $\Delta \mathcal{N}$ . Although the detailed numbers entering into eq.(29) are then quite different from those obtained with linear mixing, the resulting values of  $x_1$  were again  $\approx 0.15$  to  $0.2$ , confirming thus the estimate  $x_1 \approx 0.18$ . In view of its uncertainty, this estimate is presumably compatible with the lower end  $x_1 \approx 0.23$  of phenomenological analyses, but it seems very hard to reconcile it with the prediction  $x_1 = (1 - \beta)/2 = 0.34$  of eqs.(6,7).

Estimates of  $T_c(N)$  are shown in fig.7. More precisely, this is a log-log plot showing  $(T_\Theta - T_c(N))/T_c(N)$  against  $N$ . We see a very clean scaling law with exponent  $x_3 = 0.51 \pm 0.01$ , suggesting that the mean field value  $1/2$  is indeed correct. We should however realize that we are not yet very far in the scaling regime, in spite of the large values of  $N$ . Thus, using slightly different scaling variables as, e.g.,  $(T_\Theta - T_c(N))/T_\Theta$  instead of the variable used in fig.7, might lead to slightly different exponents. Also, this plot is very sensitive to the exact value of  $T_\Theta$ . In order to reduce this uncertainty further, we have made additional simulations of single very long polymer chains using the same routine as in [22], but with even larger  $N$  (up to  $1.6 \times 10^6$ ) and even larger system sizes (up to  $512^3$  sites). Our best estimate is now  $T_\Theta = 3.717 \pm 0.002$ . This uncertainty contributes less than  $0.01$  to the uncertainty of  $x_3$ . Finally, according to eq.(17) we should see weak logarithmic corrections. We believe that we do not see them in fig.7 because of the just mentioned uncertainties. In summary, we can say that  $x_3 = 1/2$  is the most likely value.

Finally, in fig.8 we show our estimates of the critical density. For our largest values of  $N$  (which agree roughly with the longest chains used in experiments) we see a power law with exponent  $x_2 \approx 0.38$ . This agrees perfectly with experiment and with phenomenological analyses [5]-[11]. If we accept this as the true critical exponent, and accept at the same time the mean field exponent  $y = 1$ , we run into the problem posed by inequality (19). But we see also from fig.8 that there are very large corrections to scaling. If we define effective  $N$ -dependent exponents by fitting locally, they increase slightly but systematically with  $N$ .

This suggests strongly that the deviation from the mean field exponent  $x_2 = 1/2$  is entirely due to finite- $N$  corrections which vanish for  $N \rightarrow \infty$ . This is completely consistent with the very large non-asymptotic corrections seen for single chains in the limit  $N \rightarrow \infty$  in [21, 22]. To stress the similarity between the critical monomer density  $\phi_c(N)$  as a function of  $T_c(N)$ , and the infinite chain density  $\phi_\infty$  at the same value of the temperature, we plot them both in fig.9. We see nearly parallel curves which suggests that indeed both densities scale with the same power of  $T_\Theta - T$ . For the same values of  $T$ , Flory-Huggins theory predicts  $\phi_\infty/\phi_c = 3$ . For the longest chains our data give  $3.2 \pm 0.2$  for this ratio, with a slight tendency to increase with  $N$ . We see the same small curvature in both curves, suggesting that a pure power fit might not be appropriate. Such a fit would give an exponent  $0.75$  to  $0.85$ , depending on the interval used for the fit. The dashed line indicates in contrast the prediction of eq.(18). It does not give a perfect fit, but it definitely shows the correct trend. In particular, fitting this curve

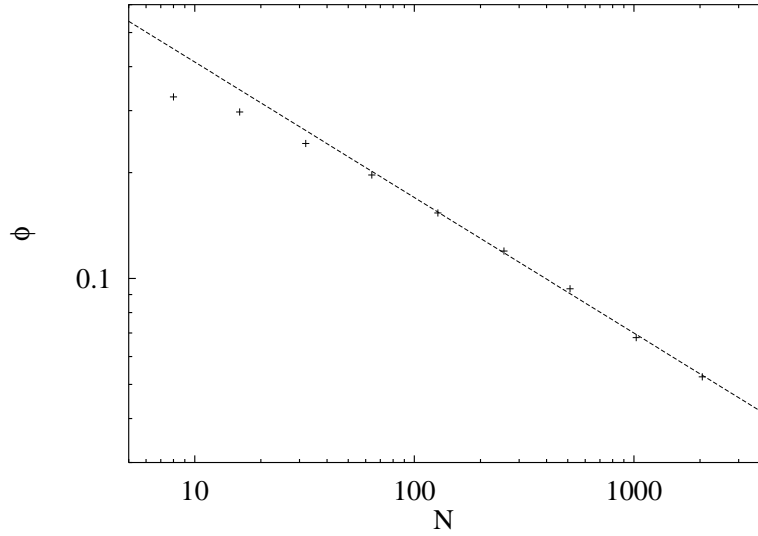


Figure 8: Log-log plot of  $\phi_c(N)$  against  $N$ . The dashed line has slope  $-0.385$ . It fits the data for large  $N$ , but there are very substantial deviations at small  $N$ .

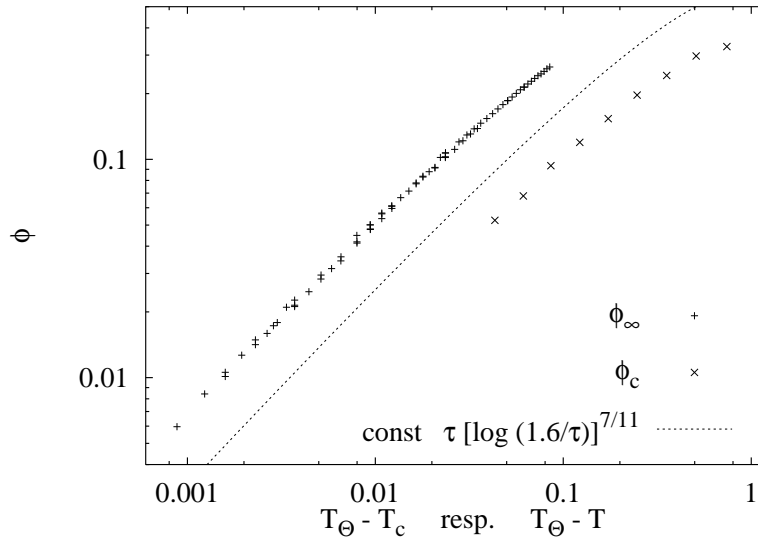


Figure 9: Double logarithmic plots of the infinite- $N$  monomer density  $\phi_\infty$  and of the critical densities for finite  $N$ , as functions of  $T_\Theta - T$  resp.  $T_\Theta - T_c(N)$ . The values for  $\phi_\infty$  are mostly from [22], except for the points very close to  $T_\Theta$ . The slight scatter of these points reflects the dependence on system size. The dashed line corresponds to eq.(18), with  $\tau = (T_\Theta - T)/T$ , and with  $\log \tau$  arbitrarily replaced by  $\log 1.6\tau$ .

by a pure power law would give an exponent  $\approx 0.8$  to  $0.9$  (again depending on the fit interval), while the correct power is 1. It seems thus very likely that all deviations from mean field behavior seen in figs. 8 and 9 are due to logarithmic corrections.

It seems thus likely that Flory-Huggins theory provides a much better description

of unmixing of long polymer chains than previously thought. To check this directly, we tested the ansatz eq.(2) directly. According to it, the free energy for fixed volume and temperature should consist of a term which depends only on the monomer density  $\phi$ , plus a *known* entropy contribution which also depends on the chain length  $N$ . To test this, we made simulations at the same  $T$  ( $= 3.5631$ ) and in the same volume ( $128^3$  sites) for chain lengths  $N = 1024, 2048$ , and  $4096$ . Within statistical errors, this  $T$  is the critical temperature for  $N = 2048$ , thus the chains with  $N = 1024$  are deeply in the single-phase domain, while those for  $N = 4096$  are deeply in the two-phase region. This is illustrated in fig.10a. There, constants are added arbitrarily, and fugacities are adjusted arbitrarily such that the curves are flattest in a qualitative sense.

In fig.10b we show the same data, but after removing the supposed entropic contribution  $-N^{-1}V\phi \log \phi$ . In this panel, additive constants and fugacities are adjusted such that the curves coincide for large  $\phi$ . It is there where eq.(2) should be most reliable: for large monomer densities, where chains penetrate substantially, there should be hardly any difference between one chain of length  $N$  and two chains of length  $N/2$ , up to the entropic difference which is taken out in fig.10b. The non-trivial hypothesis underlying eq.(2) is that the same is true also for small densities. We see from fig.10b that it is not perfectly true, but the  $N$ -dependence in fig.10b is much weaker than that in fig.10a. A detailed fit shows in addition that none of the curves in fig.10b can be fitted perfectly by a cubic polynomial, showing that the internal energy contains also terms  $\sim \phi^4$  and, since this term has the wrong sign, higher powers.

Thus the Flory-Huggins ansatz is not exact, but it seems to be a good first approximation. We should expect deviations from Flory-Huggins due to logarithmic corrections, as discussed in sec.1. As pointed out there, the leading corrections preserve eq.(2), whence also  $\phi_\infty = 3\phi_c$  should still hold. But the coefficients of the quadratic and cubic terms,  $v$  and  $w$ , should decrease slowly with  $N$ . This is indeed found when making power law fits to the curves in fig.10b (both decrease roughly by 20% when going from  $N = 1024$  to  $4096$ ), but we cannot make a more detailed comparison because of the presence of higher than cubic terms.

## 5 Discussion

We have applied a novel Monte Carlo scheme to simulate very large systems of chain polymers in semidilute solutions. Our system sizes are comparable to those of previous analyses as far as chain numbers are concerned. But our chain lengths are *much* longer, extending to  $> 2000$ . The latter would have been unfeasible for other algorithms we are aware of, and is possible only since our algorithm can make use of the fact that long chains close to the critical point are nearly free.

Our most solid result is that chains at the critical unmixing point are not shrunk. They are slightly expanded, but the expansion factor tends to a constant for chain length  $N \rightarrow \infty$ . Thus asymptotically, for  $N \rightarrow \infty$ , chains are Gaussian in contrast to recent speculations, but in agreement with the most recent simulations [18]. A somewhat less strong result which, however, seems also very clear cut, is that the  $N$ -

dependence of the critical temperatures is as predicted by Flory-Huggins (mean field) theory. Again this is in contrast to recent speculations.

Strong deviations from mean field behavior were seen in the critical density  $\phi_c$ . Here, a scaling fit would produce the same anomalous critical exponent as seen also in experiment. But we show that  $\phi_c$  can obey this seen anomalous scaling *only* if the *same* anomalous scaling governs also the density inside a very large globule, i.e. a single

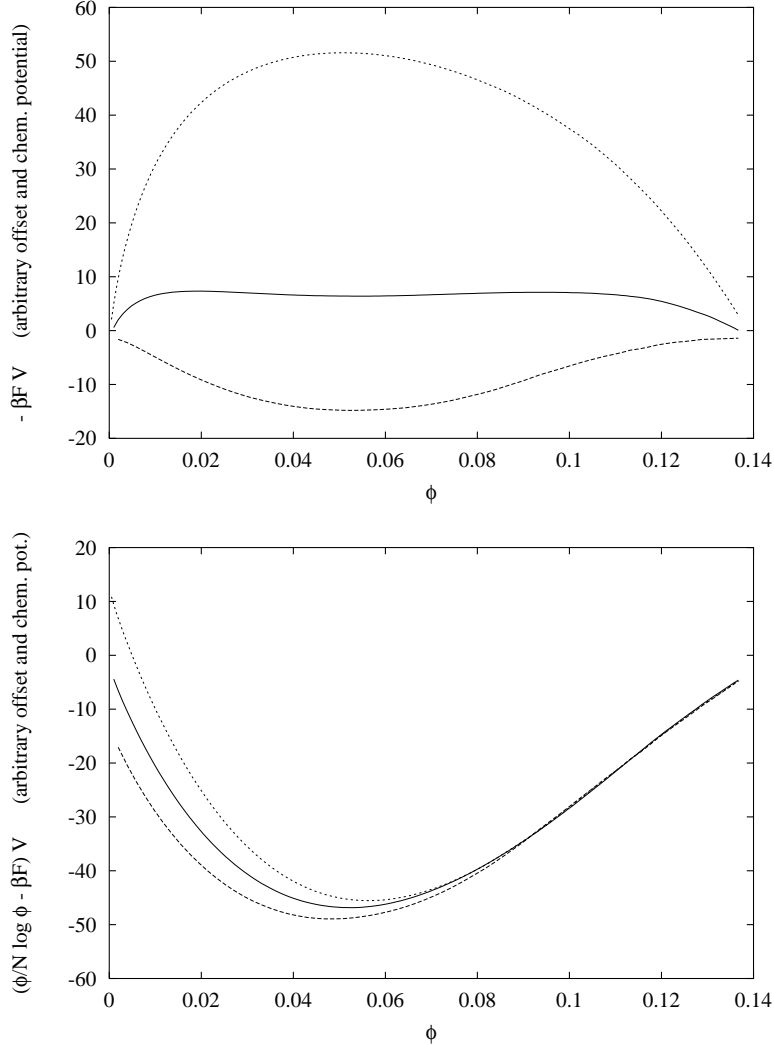


Figure 10: (a) Total negative free energy  $-\beta F V$  of systems with three different chain lengths (upper curve:  $N = 1024$ ; middle curve:  $N = 2048$ ; lower curve:  $N = 4096$ ) plotted against the monomer concentration  $\phi$ . In all three cases, lattice size and temperature were the same:  $V = 2^{21}$  sites, and  $T = 3.5631$ . The latter is close to  $T_c$  for  $N = 2048$ , while chains with  $N = 1024$  ( $4096$ ) are in the single phase (coexistence) domains. (b)  $(\phi/N \log \phi - \beta F) V$  for the same systems as in panel a. According to the Flory-Huggins ansatz, this should be independent of  $N$ . Fugacities and additive constants are fixed such that the curves coincide for large  $\phi$ .

collapsed polymer chain close to the  $\Theta$  point. For the latter, a superficial analysis also suggests anomalous scaling. But theoretical prejudices and more careful simulations suggest these might be fake and due to large logarithmic corrections to scaling. These corrections are in qualitative agreement with field theoretic predictions, and should vanish at extremely large chain lengths and extremely close to the  $\Theta$  point.

Our simulations do not suggest that deviations from mean field behavior — which must be present because of the anomalous Ising exponents — are “minimal” in the sense of de Gennes [2]: in contrast to the prediction  $x_1 = (1 - \beta)/2 = 0.34$  (where  $x_1$  the exponent for the  $N$ -dependence of the order parameter) we find  $x \approx 0.18$ , even lower than most phenomenological estimates. But we should say that this estimate is by far the most shaky of all our results.

It is not clear whether our predictions can be tested by new experiments or by re-analyzing old ones. Our chain lengths are comparable to those in real experiments ( $\approx 1000$  Kuhnian lengths), and we predict that mean field behavior should be seen in  $\phi_c$  only for *much* longer chains. This seems not feasible at present. On the other hand, fits involving the logarithmic corrections might show their presence already for shorter chains. Measurements of  $T_c(N)$  and of chain dimensions could be improved, and should be in agreement with mean field behavior since logarithmic corrections seem to be small for them.

The biggest problem in simulations are the finite sizes of the system. In contrast to chain lengths, chain numbers in our simulations are orders of magnitude smaller than those in real experiments. Nevertheless we believe that finite size effects do not seriously affect our conclusions. This is due to the use of sophisticated histogram methods [23] which allow a detailed comparison with the finite size behavior of the Ising model. Essentially they make scaling ansatzes for the microcanonical partition sum (a similar method, but without the correct finite size dependence of the microcanonical partition sum, was proposed in [38]). We verified this dependence partially, which means in particular that we also measured the Ising exponents  $\beta$  and  $\nu$  within our simulations. But we found that the simple linear field mixing proposed in [23, 18] does not work particularly well. We showed that a nonlinear mixing ansatz works much better, but we have no good theoretical reason for this ansatz. This is an interesting problem which deserves further investigations. But it is not very important as far as the precise location of the critical point and the extraction of critical parameters are concerned (except for the exponent  $x_1$ ), and it cannot affect the above conclusions.

### **Acknowledgement:**

We thank many colleagues for discussions, mainly Gerard Barkema, Ugo Bastolla, Bertrand Duplantier, Walter Nadler, and Lothar Schäfer. We are also indebted to Nigel Wilding for correspondence.

## References

- [1] P.J. Flory, *Principles of Polymer Chemistry* (Cornell Univ. Press, Ithaca, 1953) Ch. XIII
- [2] P.G. de Gennes, *Scaling Concepts in Polymer Physics* (Cornell Univ. Press, Ithaca, 1979)
- [3] B. Widom, *Physica A* **194**, 532 (1993)
- [4] R. Perzynski, A. Delsanti, and M. Adam, *J. Physique (Paris)* **48**, 115 (1987)
- [5] T. Dobashi, M. Nakata, and M. Kaneko, *J. Chem. Phys.* **72**, 6685, 6692 (1980)
- [6] K. Shinozaki, T.V. Tan, Y. Saito, and T. Nose, *Polymer* **23**, 728 (1982)
- [7] B. Chu and Z. Wang, *Macromolecules* **21**, 2283 (1988)
- [8] K.-Q. Xia, C. Franck, and B. Widom, *J. Chem. Phys.* **97**, 1446 (1992)
- [9] Y. Izumi and Y. Miyake, *J. Chem. Phys.* **81**, 1501 (1984)
- [10] I.C. Sanchez, *J. Appl. Phys.* **58**, 2871 (1985)
- [11] I.C. Sanchez, *J. Phys. Chem.* **93**, 6983 (1989)
- [12] S. Enders, B.A. Wolf, and K. Binder, *J. Chem. Phys.* **103**, 3809 (1995)
- [13] M. Muthukumar, *J. Chem. Phys.* **85**, 4772 (1986)
- [14] S. Stepanow, *J. Physique (Paris)* **48**, 2037 (1987)
- [15] A.L. Kholodenko and C. Quian, *Phys. Rev. B* **40**, 2477 (1989)
- [16] B.J. Cherayil, *J. Chem. Phys.* **95**, 2135 (1991); *J. Chem. Phys.* **98**, 9126 (1993)
- [17] D. L'Huillier, *J. Physique (Paris)* **II 2**, 1411 (1992); **3**, 547 (1993)
- [18] N.B. Wilding, M. Müller, and K. Binder, *J. Chem. Phys.* **105**, 802 (1996)
- [19] B. Duplantier, *J. Physique (Paris)* **43**, 991 (1982)
- [20] B. Duplantier, *J. Chem. Phys.* **86**, 4233 (1997)
- [21] P. Grassberger and R. Hegger, *J. Chem. Phys.* **102**, 6681 (1995)
- [22] P. Grassberger, to be published in *Phys. Rev. E* (1997)
- [23] N.B. Wilding and A.D. Bruce, *J. Phys. C* **4**, 3087 (1992)
- [24] N.B. Wilding and M. Müller, *J. Chem. Phys.* **102**, 2562 (1995)

- [25] J.J. Rehr and N.D. Mermin, Phys. Rev. **A 8**, 472 (1973)
- [26] M.N. Rosenbluth and A.W. Rosenbluth, J. Chem. Phys. **23**, 356 (1955)
- [27] F.T. Wall and J.J. Erpenbeck, J. Chem. Phys. **30**, 634, 637 (1959)
- [28] J. Batoulis and K. Kremer, J. Phys. **A 21**, 127 (1988)
- [29] T. Garel and H. Orland, J. Phys. **A 23**, L621 (1990)
- [30] B. Velikson, T. Garel, J.-C. Niel, H. Orland, and J.C. Smith, J. Comput. Chem. **13**, 1216 (1992)
- [31] U. Bastolla and P. Grassberger, preprint cond-mat 9705178 (1997)
- [32] H. Frauenkron, U. Bastolla, E. Gerstner, P. Grassberger, and W. Nadler, preprint cond-mat 9705146 (1997)
- [33] H.W.J. Blöte, E. Luitjen, and J.R. Heringa, J. Phys. **A 28**, 6289 (1995)
- [34] A.L. Talapov and H.W.J. Blöte, preprint cond-mat 9603013 (1996)
- [35] W.G. Madden, A.I. Pesci, and K.F. Freed, Macromolecules **23**, 1181 (1990)
- [36] A.D. Mackie, A.Z. Panagiotopoulos, and S.K. Kumar, J. Chem. Phys. **102**, 1014 (1995)
- [37] Q. Yan, H. Liu, and Y. Hu, Macromolecules **29**, 4066 (1996)
- [38] A. Hüller, Z. Physik **B 93**, 401 (1994)